Hydrological cycle changes explain weak Snowball Earth storm track despite increased surface baroclinicity

T. A. Shaw[1] and R. J. Graham[2]

[1]Department of the Geophysical Sciences, The University of Chicago, Chicago, IL, 60637
[2]Department of Physics, The University of Oxford, Oxford, UK

Key Points:

- Weak Snowball Earth storm track consistent with decreased gradient of latent heat flux and shortwave absorption and Clausius-Clapeyron.
- Weak storm track also consistent with decreased latent heat release aloft in the tropics, which weakens Mean Available Potential Energy.
- Both mechanisms reflected in the significant correlation between storm track intensity and surface moist static energy gradient.

Corresponding author: Tiffany A. Shaw, tas1@uchicago.edu

This article has been accepted for publication and undergone full peer review but has not been through the copyediting, typesetting, pagination and proofreading process which may lead to differences between this version and the Version of Record. Please cite this article as doi: 10.1029/2020GL088653

Abstract

Simulations show storm tracks were weaker during past cold, icy climates relative to the modern climate despite increased surface baroclinicity. Previous work explained the weak North Atlantic storm track during the Last Glacial Maximum using dry zonally-asymmetric mechanisms associated with orographic forcing. Here we show zonally-symmetric mechanisms associated with the hydrological cycle explain the weak Snowball Earth storm track. The weak storm track is consistent with the decreased meridional gradient of evaporation and atmospheric shortwave absorption and can be predicted following global-mean cooling and the Clausius-Clapeyron relation. The weak storm track is also consistent with decreased latent heat release aloft in the tropics, which decreases upper-tropospheric baroclinicity and Mean Available Potential Energy. Overall, both hydrological cycle mechanisms are reflected in the significant correlation between storm track intensity and the meridional surface moist static energy gradient across a range of simulated climates between modern and Snowball Earth.

Plain Language Summary

Storm tracks (low and high pressure weather systems) dominate Earth's climate in the middle latitudes. Several modern theories connect storm track intensity to the equator-to-pole near-surface temperature gradient. However, it has been known for some time that this connection fails when applied to simulations of past cold, icy climates such as the Last Glacial Maximum and Snowball Earth. Previous work explained the weak North Atlantic storm track during the Last Glacial Maximum using dry longitudinally-dependent dynamical mechanisms associated with orographic forcing. Here we show the weak Snowball Earth storm track can be explained by hydrological cycle changes that are independent of longitude. In particular, the weak storm track is consistent with the decreased equator-to-pole gradient of evaporation, absorption of sunlight and surface moist static energy, which follow global-mean cooling and the Clausius-Clapeyron relation. The decreased equator-to-pole surface moist static energy gradient is correlated with decreased latent heat release aloft in the tropics, which weakens the potential energy that is available to be converted into kinetic energy.

1 Introduction

Storm tracks are regions where midlatitude cyclones occur most frequently and several modern theories connect their intensity to (near-) surface baroclinicity (meridional temperature gradient, Chang et al., 2002; Shaw et al., 2016; Held, 2018). The surface baroclinicity-intensity connection is supported by the seasonality of storm track intensity in modern reanalysis data (see Fig. S5 in O'Gorman, 2010) and idealized simulations of annual-mean storm track intensity across a range of climates without ice (see Fig. 4 in O'Gorman & Schneider, 2008) (see Fig. 1 in Caballero & Langen, 2015). It is also assumed in Energy Balance Models (EBMs) based on surface temperature (North, 1975; Mbengue & Schneider, 2018) and surface moist static energy (Frierson et al., 2007). However, it has been known for some time that the surface baroclinicity-intensity connection fails when applied to simulations of past cold, icy climates such as the Last Glacial Maximum (LGM, Hall et al., 1996; Li & Battisti, 2008) and Snowball Earth (Pierrehumbert, 2005). The Snowball Earth hypothesis proposes that during Neoproterozoic glaciations ice covered most of the planet, possibly to the equator (Hoffman et al., 2017).

Several mechanisms have been proposed to explain why the Northern Hemisphere (NH) wintertime Atlantic storm track during the LGM is weaker than modern despite increased surface baroclinicity. All of the mechanisms are based on dry zonally-asymmetric dynamics, e.g. they appeal to changes in stationary wave amplitude (Hall et al., 1996), reflection (Lofverstrom et al., 2016) and structure (Riviere et al., 2018) due to the orographic forcing of the continental ice sheets or changes in upstream seeding (Donohoe

& Battisti, 2009). Zonal-asymmetries are weaker in Snowball Earth simulations (Graham et al., 2019), however the weakening of the NH wintertime zonal-mean Snowball Earth storm track is too large (∼4 PW, see Fig. 7 in Pierrehumbert, 2005) to be explained by zonally-asymmetric LGM mechanisms. Thus, alternative mechanisms are needed.

The hydrological cycle offers alternative zonally-symmetric mechanisms to explain the weak Snowball Earth storm track despite increased surface baroclinicity. The cold, icy Snowball Earth conditions decrease latent heat release aloft, decrease evaporation and increase surface albedo. The decrease of latent heat release aloft affects atmospheric thermal structure (static stability and meridional temperature gradient aloft) and Mean Available Potential Energy (MAPE), which impacts storm track intensity as measured by eddy kinetic energy (EKE). O'Gorman and Schneider (2008); Schneider et al. (2010) showed storm track intensity changes from warm and wet to cold and dry climates in idealized simulations were controlled primarily through the impact of latent heat release on static stability. Thus, the weak Snowball Earth storm track may be connected to static stability changes rather than surface baroclinicity changes. However, Yuval and Kaspi (2020) showed static stability changes can oppose surface baroclinicity resulting in a small net storm track intensity change in dry idealized simulations, highlighting the difficulty of predicting storm track changes based on static stability alone.

The transition from ocean and land to ice everywhere decreases evaporation (surface latent heat flux) and increases surface albedo, which affects the Moist Static Energy (MSE) budget of the atmosphere. Shaw et al. (2018) developed a MSE framework for zonal-mean storm track intensity and showed the increased meridional latent heat flux gradient in response to global-mean surface warming strengthens the NH wintertime storm track. Tan and Shaw (2020) used the locking technique to confirm global-mean warming dominates the meridional latent heat flux gradient response rather than the deviation from global-mean warming, i.e. the surface baroclinicity response. Thus, the weak Snowball Earth storm track may be connected to the decreased meridional latent heat flux gradient in response to global-mean surface cooling.

Here we quantify whether zonally-symmetric mechanisms associated with the hydrological cycle can explain why the Snowball Earth storm track is weaker than modern despite increased surface baroclinicity. We simulate a hard Snowball Earth (ice everywhere) and quantify the impact of the hydrological cycle via changes in surface boundary conditions using the MSE framework and atmospheric thermal structure using MAPE. We predict a weaker Snowball Earth storm track assuming hydrological cycle changes follow global-mean cooling and the Clausius-Clapeyron relation. Finally, we quantify the connection between storm track intensity and other variables such as meridional surface MSE gradient and upper-tropospheric baroclinicity.

2 Methods

2.1 MSE framework

The MSE framework for storm track intensity can be derived from the zonal-mean atmospheric MSE budget with the global mean removed:

$$\nabla \cdot F_{TE} = \nabla \cdot F_{NE} - \nabla \cdot F_{SC} \tag{1}$$

(see (2) in Kang et al., 2008), where $F_{TE} = \langle [\overline{v'm'}] \rangle$ and $F_{SC} = \langle [\overline{v}\ \overline{m}] \rangle$ are the MSE flux by transient eddies and stationary circulation (mean meridional circulation plus stationary eddies), respectively, $\nabla \cdot F_{NE} = NE$ is in flux form where NE is the net energy input with its global mean removed, $\langle \cdot \rangle$ denotes a mass-weighted vertical integration, $[\cdot]$ denotes a zonal average and $\bar{\cdot}$ denotes a monthly average, i.e. an average over a particular month not the climatological monthly average. Similar results are obtained using a 10-day high pass filter (Shaw et al., 2018). The global mean is removed to em-

phasize meridional gradients (see Kang et al., 2008; Donohoe & Battisti, 2012; Shaw et al., 2018; Donohoe et al., 2020).

An equation for storm track intensity I (unit PW) is derived by multiplying (1) by $2\pi a^2 \cos\phi$ where a is the radius of the Earth and ϕ is latitude and integrating between the pole and the storm track position ϕ_s (where $\nabla \cdot F_{TE} = 0$):

$$I = 2\pi a \cos\phi_s F_{TE}|_{\phi_s} = I_{NE} - I_{SC} \quad (2)$$
$$= 2\pi a \cos\phi_s \left[F_{NE}|_{\phi_s} - F_{SC}|_{\phi_s}\right] \quad (3)$$

(Shaw et al., 2018). Consequently, a storm track intensity change (δI) is connected to changes in net energy input (δI_{NE}) or MSE flux by the stationary circulation (δI_{SC}):

$$\delta I = \delta I_{NE} - \delta I_{SC}. \quad (4)$$

In order to quantify and predict the impact of hydrological cycle changes on storm track intensity we decompose net energy input as follows

$$\delta I_{NE} = \delta I_{THF} + \delta I_{SWABS} - \delta I_{GHE} - \delta I_{\partial h/\partial t} \quad (5)$$
$$= 2\pi a \cos\phi_s \left[\delta F_{THF}|_{\phi_s} + \delta F_{SWABS}|_{\phi_s} - \delta F_{GHE}|_{\phi_s} - \delta F_{\partial h/\partial t}|_{\phi_s}\right] \quad (6)$$

where THF is the turbulent heat flux (sensible SH plus latent LH heat flux), SWABS is the shortwave absorption (TOA minus surface shortwave radiation), GHE is the greenhouse effect (surface minus TOA longwave radiation), $\partial h/\partial t$ is atmospheric storage where $h = c_p T + L_v q$ is specific enthalpy and all terms are written in flux form, e.g. $\nabla \cdot \delta F_{THF} = \delta THF$ and δTHF has its global mean removed. The storm track interacts with the terms on the right hand side of (6), thus it is difficult to infer causality when the MSE framework is used diagnostically. However, Shaw et al. (2018); Barpanda and Shaw (2020) showed external parameters in the MSE framework, e.g. insolation and mixed layer depth, can form the basis of predictions, scaling estimates and thereby causal understanding.

We can predict the impact of hydrological cycle changes on storm track intensity between the Snowball Earth and modern climates using the MSE framework and the Clausius-Clapeyron relation. The fractional humidity change between different climates following the Clausius-Clapeyron relation is:

$$\frac{\delta q_s^*}{q_{s,M}^*} \approx \frac{\delta e_s}{e_{s,M}} = \exp\left[\frac{L_v}{R_v}\left(\frac{\delta T}{T_S T_M}\right)\right] - 1 = \gamma \quad (7)$$

where q_s^* is the saturation specific humidity, e_s is the saturation water vapor pressure and the subscripts M and S refer to the modern and Snowball Earth climates, respectively (Held & Soden, 2006; Schneider et al., 2010; Boos, 2012). Using representative global-mean surface temperatures for the Snowball Earth ($T_S \approx 245$ K) and modern ($T_M \approx 285$ K) climates the humidity decrease implied from (7) is approximately 95% ($\gamma \approx -0.95$).

Here we predict the impact of the hydrological cycle via surface boundary condition (latent heat flux and surface albedo) changes on Snowball Earth storm track intensity. While we expect hydrological cycle changes will also impact the greenhouse effect (via a colder global-mean temperature), it is not clear how the meridional structure of temperature will change because it is affected by the storm track itself. Thus, we cannot easily predict δI_{GHE}. Along similar lines it is not easy to predict δI_{SC} and $\delta I_{\partial h/\partial t}$. Hence we assume δI_{GHE}, δI_{SC} and $\delta I_{\partial h/\partial t}$ are small and focus on predicting δI_{THF} and δI_{SWABS}. We use the simulations discussed below to justify our assumptions and test our predictions by diagnosing all the terms in the MSE framework.

Assuming the change in turbulent heat flux between the Snowball Earth and modern climates is dominated by latent heat flux and the latent heat flux follows changes

in saturation specific humidity then

$$\delta THF = \delta(LH + SH) \approx \delta LH \tag{8}$$

$$\frac{\delta LH_p}{LH_M} \approx \frac{\delta q_s^*}{q_{s,M}^*} - \frac{\delta H}{(1 - H_M)} \approx \frac{\delta q_s^*}{q_{s,M}^*} = \gamma \tag{9}$$

where the p subscript refers to prediction and H is relative humidity (Schneider et al., 2010). The predicted intensity change is

$$\delta I_{THF,p} = 2\pi a \cos\phi_s \delta F_{LH,p}|_{\phi_s} \tag{10}$$

where $\nabla \cdot \delta F_{LH,p} = \delta LH_p$ and δLH_p has its global mean removed. Since $\gamma < 0$ the meridional gradient of δLH_p is positive (Supplementary Fig. 1a,b) implying $\delta I_{THF,p} < 0$, i.e. a weakening of the storm track.

Shortwave absorption depends on downward TOA ($S_T^\downarrow$) and surface ($S_S^\downarrow$) shortwave radiation and the surface (α_s) and planetary (α_p) albedos, i.e. $SWABS = (1-\alpha_p)S_T^\downarrow - (1-\alpha_s)S_S^\downarrow$. Assuming Snowball Earth shortwave absorption depends on surface ice albedo, shortwave optical depth [$\tau_S = -\ln(S_{S,S}^\downarrow / S_{T,S}^\downarrow)$], and unchanged TOA shortwave radiation, i.e. $SWABS_S = (1 - e^{-2\tau_S}\alpha_{s,S})S_{T,M}^\downarrow - (1-\alpha_{s,S})e^{-\tau_S}S_{T,M}^\downarrow$, then

$$\delta SWABS_p = -(\alpha_{s,S}e^{-2\tau_S} - \alpha_{p,M})S_{T,M}^\downarrow - (1-\alpha_{s,S})e^{-\tau_S}S_{T,M}^\downarrow + (1-\alpha_{s,M})S_{S,M}^\downarrow \tag{11}$$

The predicted intensity change is

$$\delta I_{SWABS,p} = 2\pi a \cos\phi_s \delta F_{SWABS,p}|_{\phi_s} \tag{12}$$

where $\nabla \cdot \delta F_{SWABS,p} = \delta SWABS_p$ and $\delta SWABS_p$ has its global mean removed. If we assume the Snowball Earth shortwave optical depth decreases following the Clausius-Clapeyron relation, i.e. $\tau_S \approx (1+\gamma)\tau_M = 0.05\tau_M$, and the surface ice albedo is $\alpha_{s,S} = 0.6$ in AGCM and $\alpha_{s,S} = 0.8$ in AQUA then the meridional gradient of $\delta SWABS_p$ is positive (Supplementary Fig. 1c,d) implying $\delta I_{SWABS,p} < 0$, i.e. a weakening of the storm track. We note $\delta SWABS_p$ is dominated by the change in shortwave optical depth. For both predictions (10) and (12) the storm track position is assumed to be fixed to its modern value following previous work (Shaw et al., 2018).

2.2 MAPE framework

Storm track intensity defined using EKE is linearly related to MAPE in idealized simulations and reanalysis data (O'Gorman & Schneider, 2008; O'Gorman, 2010; Gertler & O'Gorman, 2019). In the simulations discussed in section 2.3, EKE is linearly related to MAPE, which we define following equation (3) in O'Gorman and Schneider (2008):

$$MAPE = \frac{\kappa c_p}{2g}\frac{1}{p_0^\kappa}\int_{p_t}^{850\text{hPa}} \{\overline{p}\}^{-(1-\kappa)} \left(-\left\{\partial_p \overline{\theta}\right\}\right)^{-1} \left(\{\overline{\theta}^2\} - \{\overline{\theta}\}^2\right) dp \tag{13}$$

where $\kappa = R/c_p$, R is dry gas constant, c_p is specific heat at constant pressure, g is gravitational acceleration, $p_0 = 1000$ hPa is a reference pressure, $\{\cdot\}$ is an average over the NH extratropics (20° to 90°N), p_t is the WMO tropopause pressure, and θ is potential temperature. We integrate from 850 hPa to p_t because it yields good agreement with the parcel moving algorithm of Stansifer et al. (2017, see Supplementary Fig. 2).

Following O'Gorman and Schneider (2008) we approximate the variance as $\left\{\overline{\theta}^2\right\} - \left\{\overline{\theta}\right\}^2 \approx \left\{\partial_y \overline{\theta}\right\}^2 L_Z^2/12$ where $\partial_y(\cdot) \equiv \partial(\cdot)/\partial\phi/a$ is the meridional gradient in spherical coordinates and L_Z is the meridional width of the baroclinic zone. Accordingly, MAPE is approximated as

$$MAPE \approx \frac{\kappa c_p}{24g}\frac{1}{p_0^\kappa}\int_{p_t}^{850\text{hPa}} \{\overline{p}\}^{-(1-\kappa)} \left(-\left\{\partial_p \overline{\theta}\right\}\right)^{-1} \left\{\partial_y \overline{\theta}\right\}^2 L_Z^2 \, dp \tag{14}$$

and changes can be decomposed into baroclinicity (δBaro.) and stability (δStab.) contributions, i.e.

$$\delta MAPE \approx \underbrace{\frac{\kappa c_p}{24g}\frac{1}{p_0^\kappa}\int_{p_t}^{850\text{hPa}} \{\overline{p}\}^{-(1-\kappa)} \left(-\left\{\partial_p\overline{\theta}\right\}\right)^{-1} \delta\left\{\partial_y\overline{\theta}\right\}^2 L_Z^2 \, dp}_{\delta\text{Baro.}} + \underbrace{\frac{\kappa c_p}{24g}\frac{1}{p_0^\kappa}\int_{p_t}^{850\text{hPa}} \{\overline{p}\}^{-(1-\kappa)} \delta\left(-\left\{\partial_p\overline{\theta}\right\}^{-1}\right)\left\{\partial_y\overline{\theta}\right\}^2 L_Z^2 \, dp}_{\delta\text{Stab.}}. \quad (15)$$

Since MAPE depends on the time- and zonal-mean temperature throughout the atmosphere, it cannot be predicted a priori for Snowball Earth.

2.3 Simulations

We focus on the NH wintertime (December, January and February) storm track and simulate hard Snowball Earth and modern climates using two configurations of the ECHAM6 general circulation model (Stevens et al., 2013). The first configuration is a slab-ocean atmospheric general circulation model, hereafter referred to as AGCM. We simulate the modern climate with modern topography, obliquity, greenhouse gases (CO2 = 280 ppmv), a 50 m mixed layer depth and zero ocean energy transport. We simulate a hard Snowball Earth by imposing ice everywhere (ocean covered with sea ice and land covered with glaciers) in the modern simulation with an ice albedo of 0.6. The AGCM simulations are identical to those in Graham et al. (2019). Climate change in the AGCM is the difference of the Snowball Earth and modern simulations.

The second configuration is a slab-ocean aquaplanet general circulation model with modern obliquity, greenhouse gases, zero ocean energy transport and thermodynamic sea ice (a motionless single slab with no open water, Giorgetta et al., 2012), hereafter referred to as AQUA. The modern AQUA simulation has a 50 m mixed layer depth (Barpanda & Shaw, 2020; Donohoe et al., 2014). Here we vary the mixed layer depth as a simple way of simulating a range of climates between modern and Snowball Earth. In particular, we vary the mixed layer depth from 50 m to 5 m for a total of 14 simulations. (We use AQUA data from both wintertime hemispheres for a total of 28.) When the mixed layer depth is $\lesssim$ 20 m we obtain a hard Snowball Earth with sea ice at the equator (Supplementary Fig. 3) because the heat capacity becomes small enough to trigger a runaway ice-albedo feedback. The ice albedo is not prescribed in AQUA and can be greater than 0.6 because of the presence of snow on ice. Climate change in AQUA is the difference of Snowball Earth (15 m mixed layer depth) and modern (50 m mixed layer depth) simulations. The difference between the other mixed layer depth simulations and the modern simulation captures a range of climates between Snowball Earth and modern.

Since it is very common in the literature to perform slab-ocean aquaplanet simulations without thermodynamic sea ice (temperature can be below freezing without ice forming, Kang et al., 2008; Lee et al., 2008; Bordoni & Schneider, 2008; O'Gorman & Schneider, 2008), we perform a 15 m mixed layer depth simulation without sea ice and with a surface (ocean) albedo of 0.06 (Supplementary Fig. 4a) to quantify the importance of icy boundary conditions.

3 Results

3.1 Simulated Snowball Earth climate

Relative to the modern climate the Snowball Earth simulations have more ice (surface albedo$\geq$ 0.6, Fig. 1a), larger NH surface baroclinicity (equator minus pole surface temperature difference increases by 27 K in AGCM and 29 K in AQUA, Fig. 1b), weaker

meridional surface MSE gradient (equator minus pole MSE difference decreases by 16 K in AGCM and 23 K in AQUA, Fig. 1c), weaker stationary eddy MSE flux (Fig. 1d) and weaker storm track intensity. Storm track intensity is measured using the vertical integral of 1) transient eddy MSE flux (Fig. 1e) and 2) EKE (Fig. 1f). The decreased meridional surface MSE gradient shows moisture dominates over temperature and a similar result holds for the near-surface (850 hPa) MSE.

The importance of icy boundary conditions for the Snowball Earth climate is quantified by comparing the 15 m mixed layer depth AQUA simulations with and without sea ice. When sea ice is disabled surface baroclinicity and storm track intensity are both weaker than the modern simulation (Supplementary Fig. 4). This demonstrates a weak storm track-increased surface baroclinicity climate change can only be achieved with ice.

3.2 Impact of hydrological cycle via changes in surface boundary conditions

According to the MSE framework, the weaker AGCM Snowball Earth storm track (δI, Fig. 2a) is associated with decreased turbulent heat flux (δI_{THF}, Fig. 2a), shortwave absorption (δI_{SWABS}, Fig. 2a) and greenhouse effect ($-\delta I_{GHE}$, Fig. 2a) contributions. The weakening of the storm track due to decreased latent heat flux (δI_{LHF}, Fig. 2a) dominates over the slight strengthening from sensible heat flux (difference between δI_{THF} and δI_{LHF}, Fig. 2a). The stationary circulation contribution ($-\delta I_{SC}$, Fig. 2a) also strengthens the storm track slightly consistent with stationary eddy-storm track compensation (Manabe & Terpstra, 1974; Barpanda & Shaw, 2017, see Figs. 1d and 1e). The contribution from atmospheric storage is small ($-\delta I_{\partial h/\partial t}$, Fig. 2a). Similar results are seen throughout the NH (Supplementary Fig. 5).

The weaker AQUA Snowball Earth storm track is also consistent with decreased turbulent heat flux (δI_{THF}, Fig. 2b) and shortwave absorption (δI_{SWABS}, Fig. 2b). Latent heat flux (δI_{LHF}, Fig. 2b) also dominates over sensible heat flux (difference between δI_{THF} and δI_{LHF}, Fig. 2b). The larger shortwave absorption contribution in AQUA as compared to AGCM (compare δI_{SWABS}, Fig. 2a,b) is discussed below. The greenhouse effect contribution in AQUA is opposite of that in AGCM (compare $-\delta I_{GHE}$ Fig. 2a,b) due to land and clouds (Supplementary Fig. 6). Finally, the stationary circulation contribution in AQUA is also opposite of that in AGCM (compare $-\delta I_{SC}$, Fig. 2a,b) because it is dominated by the mean meridional circulation.

Assuming the latent heat flux response decreases following the Clausius-Clapeyron relation [$\gamma \approx -0.95$, see (10)] over predicts the simulated weakening (compare δI_{THF} to $\delta I_{THF,p}$, Fig. 2a,b). The over prediction occurs because the latent heat flux decrease is less than 95% in the Southern Hemisphere ($\gamma > -0.95$) and the change in sensible heat flux is non-negligible (Supplementary Fig. 1a,b). Assuming the shortwave optical depth decreases following the Clausius-Clapeyron relation [$\tau_S \approx 0.05\tau_M$, see (12)] and there is a surface ice albedo everywhere over predicts the simulated weakening in AGCM (compare δI_{SWABS} to $\delta I_{SWABS,p}$, Fig. 2a) but accurately predicts it in AQUA (compare δI_{SWABS} to $\delta I_{SWABS,p}$, Fig. 2b). The AGCM over prediction is once again associated with the response in the Southern Hemisphere (Supplementary Fig. 1c,d) where the decrease of summertime shortwave optical depth is less than 95% of its modern value, i.e. $\tau_S > 0.05\tau_M$, and there are important meridional changes in planetary albedo.

Across the range of climates between modern and Snowball Earth in AQUA, the storm track intensity change follows the turbulent heat flux contribution (δI_{THF}, Fig. 2c). The shortwave absorption contribution exhibits a nonlinear relationship with intensity changes (δI_{SWABS}, Fig. 2c) and the greenhouse effect contribution exhibits the opposite sign ($-\delta I_{GHE}$, Fig. 2c). Thus, turbulent heat fluxes are not only important for the weakening of the storm track between the Snowball Earth and modern climates but are also important across a range of climates in between.

Overall, the cold, icy Snowball Earth conditions decrease the meridional gradient of latent heat flux and shortwave absorption, which leads to a weaker meridional net energy input gradient and thereby a weaker storm track. The weakening can be predicted following global-mean cooling and the Clausius-Clapeyron relation and assuming a surface ice albedo everywhere because the greenhouse effect, stationary circulation, and atmospheric storage contributions are small. The weaker storm track is also consistent with weaker meridional surface (Fig. 1c) and lower tropospheric (Fig. 2d,e) MSE gradients, which also follow the Clausius-Clapeyron relation as discussed below.

3.3 Impact of hydrological cycle via changes in thermal structure

Next we examine how the cold, dry Snowball Earth conditions impact storm track intensity, as measured by EKE, via changes in atmospheric thermal structure that affect MAPE. The weaker storm track in the AGCM Snowball Earth simulation relative to modern is consistent with weaker MAPE (δMAPE, square, Fig. 3a), which is dominated by the change in baroclinicity (δBaro., square, Fig. 3a) rather than stability (δStab., square, Fig. 3a). When examining the range of climates between modern and Snowball Earth in AQUA, the storm track intensity change relative to modern is significantly correlated with MAPE ($R = 0.98$, $\delta MAPE$, Fig. 3a) and is mostly dominated by changes in baroclinicity (δBaro., Fig. 3a) rather than stability (δStrat., Fig. 3a).

Since surface baroclinicity does not account for the weaker Snowball Earth storm track relative to the modern climate (Fig. 1b), the MAPE results suggest upper-tropospheric baroclinicity is important. Indeed the temperature difference between the Snowball Earth and modern simulations involve weaker upper-tropospheric baroclinicity connected to greater tropical cooling aloft (Fig. 3b,c).

3.4 Connecting storm track intensity to other variables

The surface baroclinicity-intensity connection is appealing because it connects storm track intensity (a turbulent quantity) to surface baroclinicity (a mean quantity), which can be inferred from paleo proxy data. However, storm track intensity is not significantly correlated with surface ($R = 0.01$, Fig. 4a) or near-surface ($R = 0.20$, Fig. 4b) baroclinicity across the AQUA and AGCM simulations.

The hydrological cycle changes suggest surface latent heat flux and latent heat release aloft (upper-tropospheric baroclincity) may be more important than surface temperature. Recall, the weaker Snowball Earth storm track is consistent with a weaker meridional gradient of latent heat flux and shortwave absorption, which follow global-mean cooling and the Clausius-Clapeyron relation [see (7)-(12)]. The meridional surface MSE gradient in Snowball Earth also follows the Clausius-Clapeyron relation (Supplementary Fig. 7a). Consistently, storm track intensity is significantly correlated with equator minus pole surface MSE ($R = 0.94$, Fig. 4c) and equator minus pole surface MSE estimated from the Clausius-Clapeyron relation ($R = 0.94$, Supplementary Fig. 7b) across the AQUA and AGCM simulations. Furthermore, equator minus pole surface MSE is significantly correlated with equator minus pole surface latent heat flux ($R = 0.96$).

Storm track intensity is also significantly correlated with upper-tropospheric baroclinicity across the AQUA and AGCM simulations ($R = 0.98$, Fig. 4d). Upper-tropospheric baroclinicity is significantly correlated with equator minus pole surface MSE ($R = 0.98$) consistent with the impact of surface moisture on latent heat release aloft in the tropics via moist adiabatic adjustment (Supplementary Fig. 7c). Upper-tropospheric and surface baroclinicity are not significantly correlated ($R = 0.10$). Note that in midlatitudes the storm track itself shapes the temperature structure aloft in addition to convection.

Overall, the meridional surface MSE gradient encapsulates both mechanisms associated with hydrological cycle changes between the Snowball Earth and modern cli-

mates. The significant correlation between storm track intensity metrics (transient eddy MSE flux or EKE) and the meridional surface MSE gradient shows surface moisture changes are important for determining Snowball Earth storm track intensity relative to the modern climate and can dominate over changes in surface baroclinicity.

4 Conclusions and Discussion

Snowball Earth is an exotic climate with a radically different hydrological cycle than the modern Earth. Here we examined whether zonally-symmetric mechanisms associated with the hydrological cycle can account for the weaker Snowball Earth storm track despite increased surface baroclinicity. The results show the weak Snowball Earth storm track is consistent with the decreased meridional gradient of turbulent heat flux (evaporation) and shortwave absorption (shortwave optical depth), which decreases the meridional gradient of net energy input. The weaker storm track can be predicted assuming a surface ice albedo everywhere and the hydrological cycle changes follow global-mean cooling and the Clausius-Clapeyron relation. The weaker storm track is also consistent with decreased latent heat release aloft in the tropics, which decreases MAPE and upper-tropospheric baroclinicity via convective adjustment. Overall, both mechanisms (decreased meridional gradient of latent heat flux and shortwave absorption and decreased latent heat release aloft) are reflected in the significant correlation between storm track intensity and the meridional surface MSE gradient across a range of climates between Snowball Earth and modern. They are also reflected in the significant correlation between storm track intensity defined using transient eddy MSE flux or EKE ($R = 0.99$). Ultimately, the results show the decreased meridional surface moisture gradient between the Snowball Earth and modern climates is important for storm track intensity and dominates over increased surface baroclinicity.

Our results are consistent with Lapeyre and Held (2004) who showed lower-layer MSE (rather than lower-layer temperature) is most appropriate for diffusive models of energy transport. Since MSE transport reflects both thermodynamic (moisture) and dynamic (EKE) components, future work must focus on understanding the importance of the moisture versus EKE decrease for the decreased Snowball Earth MSE transport, including the connection to diffusivity changes. The results imply that EBMs, which connect storm track intensity to surface baroclinicity, must also include the dependence of storm track intensity on the meridional surface moisture gradient. Hence, EBMs based on the atmospheric MSE budget, i.e. an equation for surface MSE (Frierson et al., 2007; Hwang & Frierson, 2010), should be used instead of EBMs based on the TOA energy budget, i.e. an equation for surface temperature (North, 1975; Mbengue & Schneider, 2018). Finally, our results are also consistent with previous work that highlighted the importance of upper-tropospheric baroclinicity changes for the storm track intensity response to increased CO2 (O'Gorman, 2010; Harvey et al., 2015).

Here we showed zonally-symmetric changes in the hydrological cycle can explain the weak Snowball Earth storm track despite increased surface baroclinicity. Previous work explained the weak North Atlantic storm track during the LGM using dry zonally-asymmetric mechanisms connected to orographic forcing. Assessing whether hydrological cycle mechanisms can also account for the weak LGM North Atlantic storm track requires extending the MSE framework for storm track intensity to the North Atlantic basin as well as quantifying the importance of orography versus latent heat flux and surface albedo changes (cf. Roberts & Valdes, 2017), which is work in progress. If the Snowball Earth results hold for other paleoclimates then estimates of paleo surface MSE gradients (combining paleo proxy temperatures and the Clausius-Clapeyron relation) could potentially be used to estimate paleo storm track intensity.

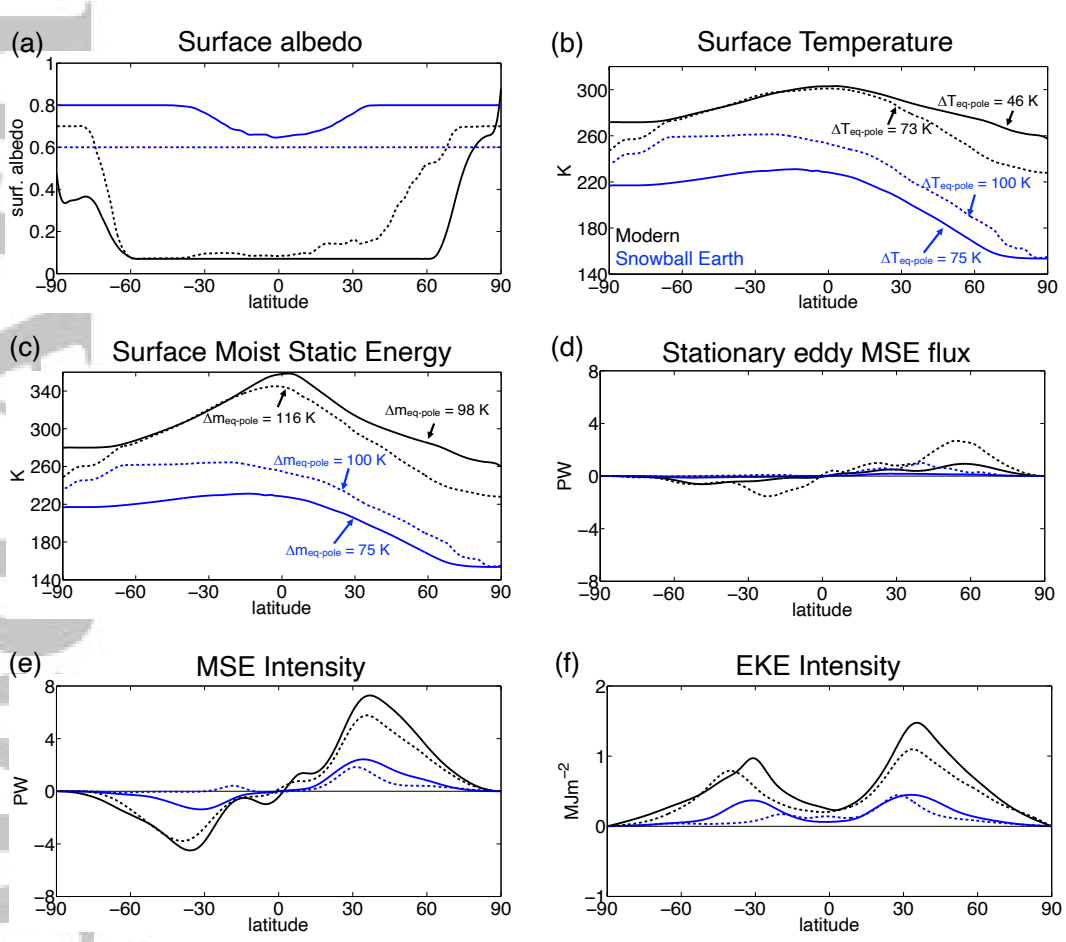

Figure 1. Northern Hemisphere wintertime (a) surface albedo, (b) surface temperature, (c) surface MSE (divided by specific heat at constant pressure), (d) stationary eddy MSE flux and storm track intensity defined by vertically-integrated (e) transient eddy MSE flux and (f) EKE for AGCM (dashed) and AQUA (solid) modern (black) and Snowball Earth (blue) simulations.

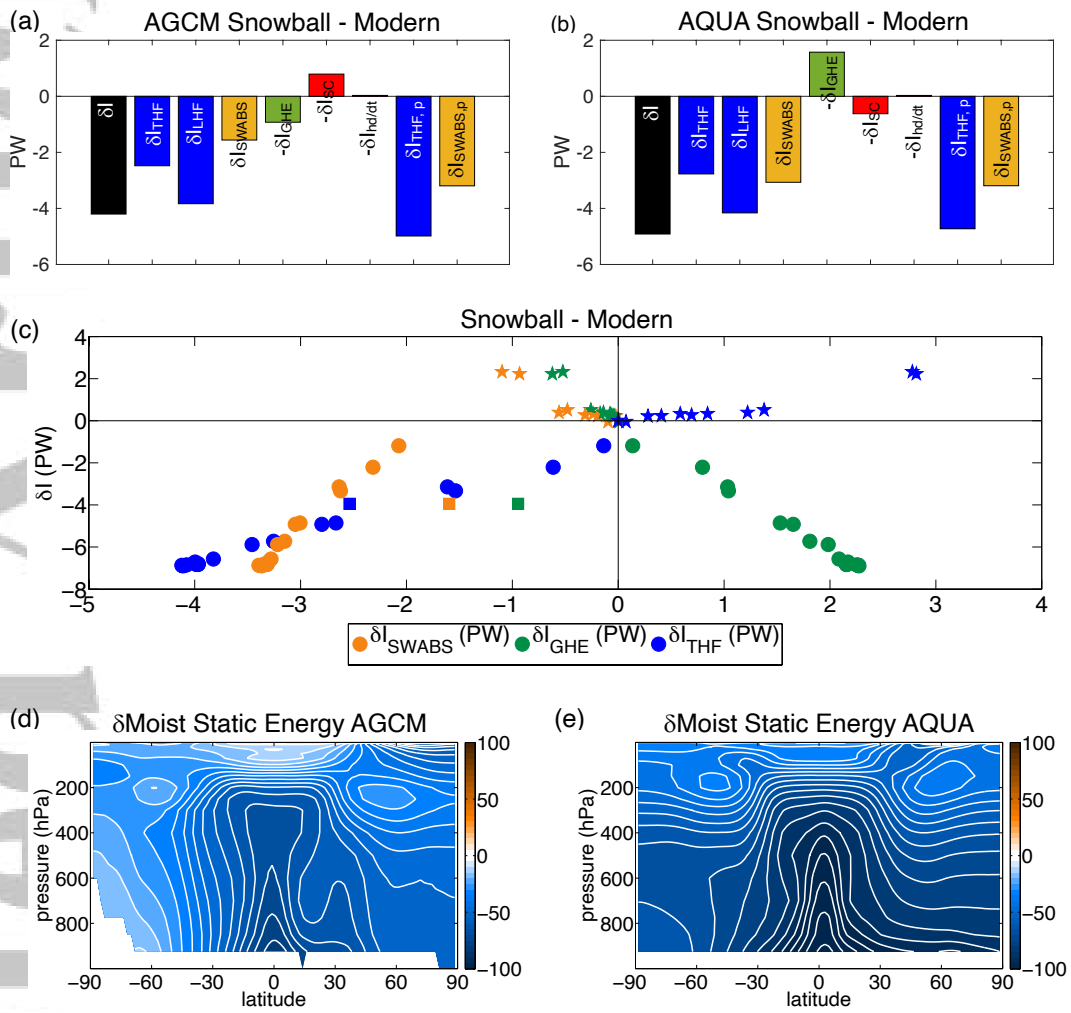

Figure 2. (a,b) Weakening of Northern Hemisphere wintertime storm track intensity between Snowball Earth and modern (δI in PW) at the storm track position decomposed into turbulent heat flux (δI_{THF}), latent heat flux (δI_{LHF}), shortwave absorption (δI_{SWABS}), greenhouse effect ($-\delta I_{GHE}$), stationary circulation ($-\delta I_{SC}$) and atmospheric storage ($-\delta I_{\partial h/\partial t}$) contributions following the MSE framework. Predicted values have a 'p' subscript. (c) The response of storm track intensity relative to modern (δI in PW) decomposed as in (a,b) across a range of simulated climates between Snowball Earth and modern. AGCM simulations shown by squares and AQUA simulations shown by stars and circles with circles denoting Snowball Earth simulations. (d,e) Difference of time- and zonal-mean MSE (divided by specific heat at constant pressure) between Snowball Earth and modern simulations. Contour interval is 5 K.

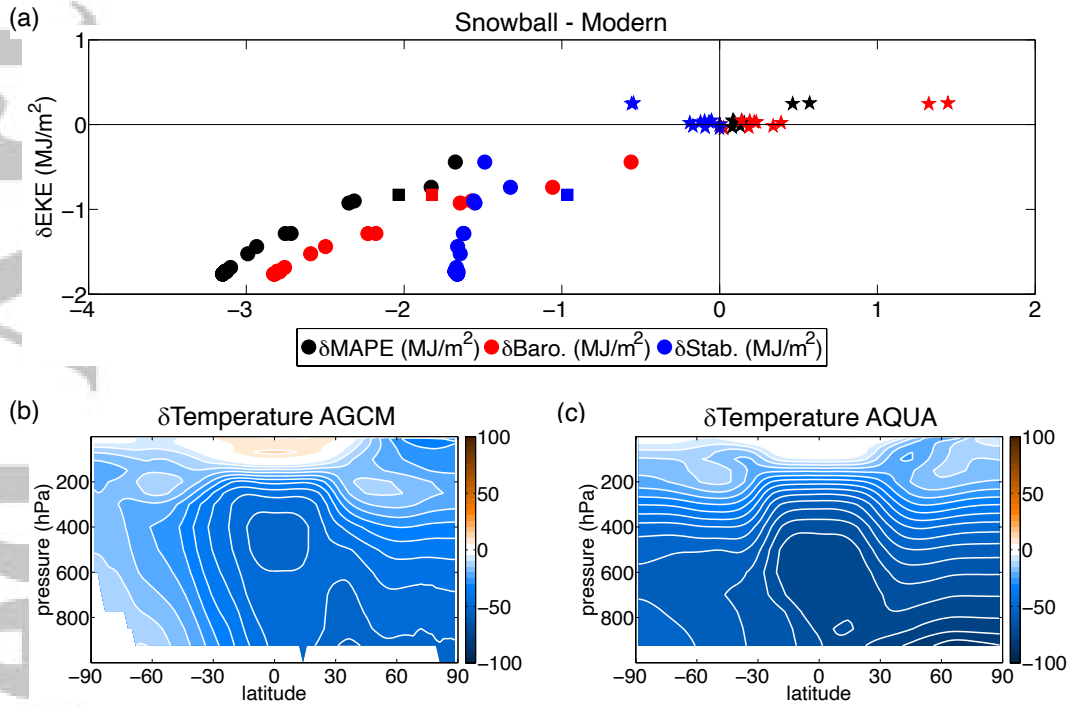

Figure 3. (a) Weakening of Northern Hemisphere wintertime EKE storm track intensity integrated over the extratropics (δEKE in MJm^{-2}) as a function of MAPE changes (δMAPE) and their decomposition into baroclinicity (δBaro.) and stability (δStab.) contributions across a range of simulated climates between Snowball Earth and modern. AGCM simulations shown by squares and AQUA simulations shown by stars and circles with circles denoting Snowball Earth simulations. (b,c) Difference of time- and zonal-mean temperature between Snowball Earth and modern simulations. Contour interval is 5 K.

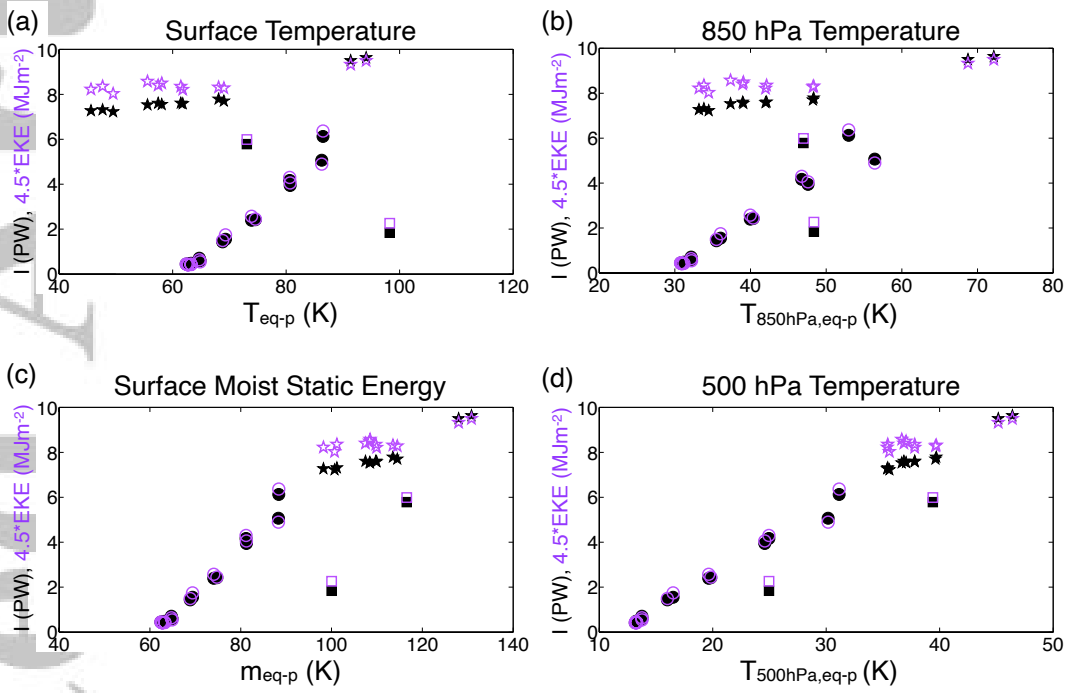

Figure 4. Storm track intensity versus equator minus pole (a) surface (2 m) temperature (b) 850 hPa temperature, (c) surface (2 m) MSE and (d) 500 hPa temperature across a range of simulated climates between Snowball Earth and modern. MSE and EKE (multiplied by 4.5) intensity indicated by black and purple symbols, respectively. AGCM simulations shown by squares and AQUA simulations shown by stars and circles with circles denoting Snowball Earth simulations.

Acknowledgments

TAS acknowledges support from NSF (AGS-1742944) and RJG acknowledges scholarship funding from the Clarendon Fund and Jesus College, Oxford. The authors thank three anonymous reviewers for their helpful comments. TAS thanks Paul O'Gorman for providing code to calculate MAPE using the parcel-moving algorithm and Osamu Miyawaki for providing code to calculate the moist adiabat. The simulations in this paper were completed with resources provided by the University of Chicago Research Computing Center. Data and code necessary to reproduce the figures in this paper are available via The University of Chicago's institutional repository Knowledge@UChicago (10.6082/uchicago.2201).

References

Barpanda, P., & Shaw, T. A. (2017). Using the moist static energy budget to understand storm-track shifts across a range of time scales. *J. Atmos. Sci.*, *74*(8), 2427–2446.

Barpanda, P., & Shaw, T. A. (2020). Surface fluxes modulate the seasonality of zonal-mean storm tracks. *J. Atmos. Sci.*, *77*, 753–779.

Boos, W. R. (2012). Thermodynamic scaling of the hydrological cycle of the Last Glacial Maximum. *J. Climate*, *25*, 992-1006.

Bordoni, S., & Schneider, T. (2008). Monsoons as eddy-mediated regime transitions of the tropical overturning circulation. *Nature Geosc.*, *1*(8), 515.

Caballero, R., & Langen, P. L. (2015). The dynamic range of poleward energy transport in an atmospheric general circulation model. *Geophys. Res. Lett.*. doi: 10.1029/2004GL021581

Chang, E., Lee, S., & Swanson, K. K. (2002). Storm track dynamics. *J. Climate*, *15*, 2163–2183.

Donohoe, A., Armour, K. C., Roe, G. H., Battisti, D. S., & Hahn, L. (2020). The partitioning of meridional heat transport from the Last Glacial Maximum to CO2 quadrupling in coupled climate models. *J. Climate*, *33*, 4793-4808.

Donohoe, A., & Battisti, D. S. (2009). Causes of reduced North Atlantic storm activity in a CAM3 simulation of the last glacial maximum. *J. Climate*, *22*, 4793-4808.

Donohoe, A., & Battisti, D. S. (2012). What determines meridional heat transport in climate models? *J. Climate*, *25*, 3832-3850.

Donohoe, A., Frierson, D. M. W., & Battisti, D. S. (2014). The effect of ocean mixed layer depth on climate in slab ocean aquaplanet experiments. *Clim. Dynamics*, *43*, 1041–1055.

Frierson, D. M. W., Held, I. M., & Zurita-Gotor, P. (2007). A gray-radiation aquaplanet moist GCM. Part II: Energy transports in altered climates. *J. Atmos. Sci.*, *64*, 1680-1693.

Gertler, C. G., & O'Gorman, P. A. (2019). Changing available energy for extratropical cyclones and associated convection in Northern Hemisphere summer. *Proc. Nat. Acad. Sci.*. doi: 10.1073/pnas.1812312116

Giorgetta, M. A., Roeckner, E., Mauritsen, T., Stevens, B., Bader, J., Crueger, T., ... Krismer, T. (2012). The atmospheric general circulation model echam6: Model description. *Max Planck Institute for Meteorology, Hamburg, Germany*. Retrieved from `https://icdc.cen.uni-hamburg.de/fileadmin/user_upload/icdc_Dokumente/ECHAM/echam6_scidoc.pdf`

Graham, R. J., Shaw, T. A., & Abbot, D. S. (2019). The snowball stratosphere. *J. Geophys. Res.*. doi: 10.1029/2019JD031361

Hall, N. M. J., Dong, B., & Valdes, P. J. (1996). Atmospheric equilibrium, instability and energy transport at the Last Glacial Maximum. *Climate Dyn.*, *12*, 197–511.

Harvey, B. J., Shaffrey, L. C., & Woollings, T. J. (2015). Deconstructing the climate change response of the Northern Hemisphere wintertime storm tracks. *Clim. Dyn.*, *45*, 2847-2860.

Held, I. M. (2018). 100 years of progress in understanding the general circulation of the atmosphere. *Meteorological Monographs*, *59*. doi: 10.1175/AMSMONOGRAPHS-D-18-0017.1

Held, I. M., & Soden, B. J. (2006). Robust responses of the hydrological cycle to global warming. *J. Climate*, *19*, 5686-5699.

Hoffman, P. F., Abbot, D. S., Ashkenazy, Y., Benn, D. I., Brocks, J. J., Cohen, P. A., ... Warren, S. G. (2017). Snowball Earth climate dynamics and cryogenian geology-geobiology. *Science Advances*. doi: 10.1126/sciadv.1600983

Hwang, Y.-T., & Frierson, D. M. W. (2010). Increasing atmospheric poleward energy transport with global warming. *Geophys. Res. Lett.*, *37*. doi: 10.2951029/

2010GL045440

Kang, S. M., Held, I. M., Frierson, D. M. W., & Zhao, M. (2008). The response of the ITCZ to extratropical thermal forcing: Idealized slab-ocean experiments with a GCM. *J. Climate*, *21*, 3521–3532.

Lapeyre, G., & Held, I. M. (2004). The role of moisture in the dynamics and energetics of turbulent baroclinic eddies. *J. Atmos. Sci.*, *61*, 1693–1710.

Lee, M.-I., Suarez, M. J., Kang, I.-S., Held, I. M., & Kim, S. (2008). A moist benchmark calculation for atmospheric general circulation models. *J. Climate*, *21*, 4934–4954.

Li, C., & Battisti, D. S. (2008). Reduced Atlantic storminess during Last Glacial Maximum: Evidence from a coupled climate model. *J. Climate*, *21*, 3561–3579.

Lofverstrom, M., Caballero, R., Nilsson, J., & Messori, G. (2016). Stationary wave reflection as a mechanism for zonalising the Atlantic winter jet at the LGM. *J. Atmos. Sci.*, *73*, 3329-3342.

Manabe, S., & Terpstra, T. B. (1974). The effects of mountains on the general circulation of the atmosphere as identified by numerical experiments. *J. Atmos. Sci.*, *31*, 3–42.

Mbengue, C., & Schneider, T. (2018). Linking Hadley circulation and storm tracks in a conceptual model of the atmospheric energy balance. *J. Atmos. Sci.*, *75*(3), 841–856.

North, J. R. (1975). Theory of energy-balance climate models. *J. Atmos. Sci.*, *32*, 1189-1204.

O'Gorman, P. A. (2010). Understanding the varied response of the extratropical storm tracks to climate change. *Proc. Nat. Acad. Sci.*, *107*, 19176–19180.

O'Gorman, P. A., & Schneider, T. (2008). Energy of midlatitude transient eddies in idealized simulations of changed climates. *J. Climate*, *21*, 5797–5806.

Pierrehumbert, R. T. (2005). Climate dynamics of a hard Snowball Earth. *J. Geophys. Res.*, *110*. doi: 10.1029/2004JD005162

Riviere, G., Berthou, S., Lapeyre, F., & Kageyama, M. (2018). On the reduced North Atlantic storminess during the last glacial period: The role of topography in shaping synoptic eddies. *J. Climate*, *31*, 1637-1638.

Roberts, W. H. G., & Valdes, P. J. (2017). Green mountains and white plains: The effect of Northern Hemisphere ice sheets on the global energy budget. *J. Climate*, *30*, 3887-3905.

Schneider, T., O'Gorman, P. A., & Levine, X. J. (2010). Water vapor and the dynamics of climate changes. *Reviews of Geophysics*, *48*. doi: 10.1029/2009RG000302

Shaw, T. A., Baldwin, M., Barnes, E. A., Caballero, R., Garfinkel, C. I., Hwang, Y.-T., ... Voigt, A. (2016). Storm track processes and the opposing influences of climate change. *Nature Geosc.*, *9*, 656–664.

Shaw, T. A., Barpanda, P., & Donohoe, A. (2018). A moist static energy framework for zonal-mean storm-track intensity. *J. Atmos. Sci.*, *75*(6), 1979–1994.

Stansifer, E. M., O'Gorman, P. A., & Holt, J. L. (2017). Accurate computation of moist available potential energy with the Munkres algorithm. *Q. J. R. Meteorol. Soc.*, *143*, 288-292.

Stevens, B., Giorgetta, M., Esch, M., Mauritian, T., Crueger, T., Rast, S., ... Roeckner, E. (2013). Atmospheric component of the MPI-M Earth System Model: ECHAM6. *J. Adv. Model. Earth Syst.*, *5*, 146–172.

Tan, Z., & Shaw, T. A. (2020). Quantifying the impact of wind and surface humidity-induced surface heat exchange on the circulation shift in response to increased CO2. *Geophys. Res. Lett.*. doi: 10.1029/2020GL088053

Yuval, J., & Kaspi, Y. (2020). Eddy activity response to global warming–like temperature changes. *J. Climate*, *33*. doi: 10.1175/JCLI-D-19-0190.1